Springer

Journal of
Mechanical
Science and
Technology

Journal of Mechanical Science and Technology 23 (2009) 3245~3256

www.springerlink.com/content/1738-494x
DOI 10.1007/s12206-009-0918-y

Analysis of the root causes of refrigerant-induced noise in refrigerators †

Hyung Suk Han[1], Weui Bong Jeong[2,*], Min Seong Kim[2] and Tae Hoon Kim[3]

[1] *1st Team, Naval Sea System Center, Defense Agency for Technology and Quality, 1, Aju-dong, Geoje, Korea*
[2] *Department of Mechanical Engineering, Pusan National University, Jangjeon-dong, Kumjung-ku, Pusan 609-735*
[3] *Engineering Design Department, LG Electronics, Gaeumjeong-dong, Changwon City,*

(Manuscript Received January 8, 2009; Revised May 7, 2009; Accepted August 26, 2009)

Abstract

Refrigerant-induced noises, which occur irregularly at special thermodynamic cycle conditions, are frequently cited by residential customers who use refrigerators. However, these noises are very difficult to resolve and their root causes cannot usually be exactly identified. In this research, the root causes of the irregular refrigerant-induced noise are estimated through the theories of two-phase flow and bubble dynamics. Also, by using refrigerant-supplying equipment that can continuously supply refrigerant to the test unit at typical cycle conditions, the flow patterns of the evaporator in vertical and horizontal pipes are inspected and their noises are simultaneously measured. Through the observation of the relationship between the flow pattern and the refrigerant-induced noise, the root causes of this irregular refrigerant noise can be identified and verified.

Keywords: 2-phase; Refrigerant-induced noise; Flow pattern map; Refrigerant-supplying equipment; Evaporator-inlet pipe; Intermittent flow; Slug flow; Churn flow; Annular flow

1. Introduction

The refrigerant-induced noise that arises in refrigerators is a noise problem in the development process of refrigerators. Since this kind of noise varies with the thermodynamic cycle conditions such as temperature, pressure and sub-cooling, the noise is very difficult to resolve. Since the overall noise level of refrigerators is decreasing nowadays, the refrigerant-induced noise becomes much more dominant. Therefore, solutions for reducing refrigerant-induced noise are urgently required. Owing to these reasons, many studies have been conducted to reduce refrigerant-induced noise.

Hirakuni [1] suggested that porous metals be installed in front of the expansion device to reduce the refrigerant-induced noise, which can change the flow pattern from slug-flow to bubbly-flow. Hirakuni [2] dealt with the refrigerant-induced noise of the refrigerator at the capillary tube. He found that the noise increased when the flow pattern was slug-flow in front of the capillary tube. He recommended the addition of a dryer in front of the capillary tube for reducing refrigerant-induced noise. Since the dryer can separate the refrigerant into liquid and vapor, the flow pattern can transform to annular flow and the refrigerant-induced noise can decrease. Umeda [3] dealt with the layout of the inlet and outlet pipes of the electric expansion valve for avoiding the slug-flow that produces the noise. He experimentally verified that the flow pattern became slug when the direction of flow of the refrigerant into the expansion valve was vertical. Therefore, he suggested that the pipe layout of the expansion valve inlet be laid horizontally. Kannon [4] dealt with the relationship between refrigerant-induced noise and the pressure variation. He experimentally verified that a transient pressure wave occurred when the vapor fraction of the refrigerant

† This paper was recommended for publication in revised form by Associate Editor Yeon June Kang

* Corresponding author. Tel.: +82 51 510 2337, Fax.: +82 51 517 3805
E-mail address: wbjeong@pusan.ac.kr

increased, at which time the noise increased. Umeda [5] investigated the refrigerant-induced noise that passes through the orifice and the relationship between the pressure variation from upstream to downstream flow and the refrigerant-induced noise. He found that the noise as well as the pressure variation increased when a large bubble passed through the orifice. Park [6] identified refrigerant-induced noise at the accumulator of refrigerators. He found that the bubble noise was produced at the sleeve that was located under the accumulator and that the noise disappeared when the orifice on the sleeve was removed.

In light of the above studies, the root causes of the refrigerant-induced noise in refrigerators can be estimated from the theories of two-phase flow and bubble dynamics. Therefore, in this research, the theories of two-phase flow and bubble dynamics are first reviewed. Based on the theories, noise and vibration tests are performed and the characteristics of noise and vibration of the refrigerator are described. Then, the variation of the flow pattern in a pipe is estimated through various flow-pattern maps that depend on the time-varying cycle conditions in the operating ranges of the refrigerator. Through a frequency analysis that is based on the bubble dynamics theory and the noise test, the relationship between the flow pattern and the noise is estimated and verified by experiments.

2. Theoretical background for the root cause of refrigerant-induced noise

In this section, the theories of two-phase flow and bubble dynamics are reviewed for estimating the root causes of the refrigerant-induced noise that arises in refrigerators.

2.1 Refrigerant-induced noise from two-phase flow theory

Figs. 1 and 2 show the schematic diagrams of the two-phase, separated-flow model. The governing equations of the separated flow model are given in Eqs. (1)~(3) [7], which are the continuity equation, energy equation, and momentum equation, respectively. In Eq. (3), the pressure drop can be represented through friction, gravity, and acceleration terms.

$$W_f + W_g = W - const. \tag{1}$$

$$-\frac{dp}{dz}(W_g v_g + W_f v_f) = W\frac{dE}{dz} + \frac{d}{dz}[\frac{1}{2}(W_f u_f^2 + W_g u_g^2)] + W_g \sin\theta \tag{2}$$

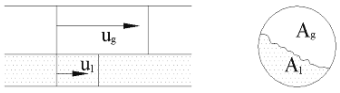

Fig. 1. Two phase flow for separated flow model.

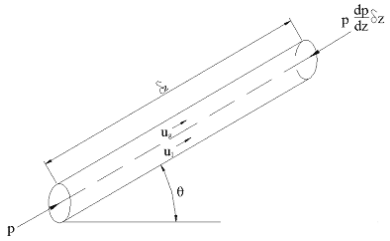

Fig. 2. Control volume of separated flow model for the momentum equation.

$$-\frac{dp}{dz} = \frac{1}{A}\frac{dF}{dz} + [(1-\alpha)\rho_f + \alpha\rho_g]g\sin\theta + \frac{W^2}{A}\frac{d}{dz}[\frac{1}{A}(\frac{x^2 v_g}{\alpha} + \frac{(1-x)^2 v_f}{1-\alpha})] = -(\frac{dp}{dz}F) - (\frac{dp}{dz}z) - (\frac{dp}{dz}a) \tag{3}$$

$$where \quad \alpha = \frac{A_g}{A}, x = \frac{W_g}{W}$$

Here, W is the mass flow rate, p is the pressure, z is the distance in the axial direction, v is the specific volume, E is the internal energy, u is the velocity, ρ is the density, α is the void fraction, x is the mass quality, θ is the angle of the pipe, A is the cross-sectional area of the pipe, A_g is the cross sectional area of the tube occupied by the gas phase, F is the shear stress on the pipe that is due to the friction, and subscripts f and g denote liquid and gas, respectively.

Through the above equations, it can be discerned that the mass quality and void fraction are time-variant terms that depend on the flow pattern in the pipe. Therefore, they can be represented as "x=x(t), α=α(t)" and the time-gradient of the pressure drop can be represented as shown in Eq. (4).

$$\frac{d}{dt}(\frac{dp}{dz}) = \frac{d}{dt}[f(x(t),\alpha(t),.....)] \tag{4}$$

From Eq. (4), it can be estimated that the time-gradient of the pressure drop should remarkably vary when the flow pattern in a pipe is intermittent, as in plug-, churn- (froth-) and slug-flows. When the flow pattern in a pipe is intermittent, the mass quality and void fraction vary irregularly over time at a particular

position. Therefore, the irregular noise and vibration can occur in the pipe because of the fluctuation in the pressure.

However, when the flow pattern in a pipe is either annular or bubbly flow, the noise level should be constant over time because the time-gradient of the pressure drop should be a very low value. This is because the mass quality and void fraction at a particular position are steady over time when the flow pattern in a pipe is either annular or bubbly flow. The flow pattern will be discussed in section 3.2 in more detail.

2.2 Refrigerant-induced noise from bubble dynamics

In this section, the bubble dynamics theories are reviewed for estimating the root cause of the refrigerant-induced noise that arises in refrigerators. Through empirical tests, Minnaert [8] suggested a relationship between bubble size and resonance frequency. Minnaert assumed the radius of the oscillating bubble, as shown in Eq. (5) [8].

$$r = r_0 + a\sin\frac{2\pi t}{T} \tag{5}$$

Here, r is the radius of the bubble, r_0 is the initial radius of the bubble, a is the amplitude of the radius of the oscillating bubble, and T is the period of oscillation.

When it is assumed that the potential energy as given in Eq. (6) is equal to the kinetic energy as given in Eq. (7), the resonance frequency of the bubble can be represented as given in Eq. (8) [8].

$$-\int_{v_0}^{v}(p-p_0)dv = \int_0^a \frac{3kpx}{r}4\pi r^2 dx = 6\pi kpra^2 \tag{6}$$

$$\frac{1}{2}\int\left(\frac{\partial r}{\partial t}\right)^2_{\max} dm = \frac{\rho}{2}\int_r^\infty \frac{r^4}{R^2}\frac{16\pi^3 a^2}{T^2}dR = \frac{8\pi^3\rho r^3 a^2}{T^2} \tag{7}$$

$$T^2 = \frac{4\pi^2\rho r^2}{3kp}, \quad \omega_n = \frac{1}{T} = \frac{1}{r}\sqrt{\frac{3kp}{\rho}} \tag{8}$$

Here, ω_n is the resonance frequency of the bubble, p_0 is the pressure inside the bubble, p is the pressure outside the bubble, and k is the specific heat ratio.

In Eq. (8), it can be found that the frequency of the bubble noise is strongly dependent on the bubble size.

Strasburg [9] experimentally found that the bubble noise occurs when the volume of the bubble changes and he suggested an equation for the bubble behavior that is represented by the volume terms, as shown in Eq. (9).

$$\frac{\rho}{4\pi r_0}\ddot{v} + R\dot{v} + \frac{kP_0}{V_0}(v - V_0) = P_0 - p_e(t) \tag{9}$$

Here, P_0 is the static pressure of the bubble at the initial volume of the bubble(V_0), $p_e(t)$ is the instantaneous external pressure, and R is the resistance coefficient that varies in a complex manner with the bubble size and frequency. In Eq. (9), R_0 is taken as the radius of sphere of the same volume if the bubble is non-spherical.

From Eq. (9), the sound pressure that is instantaneously radiated at the distance "d" can be represented as in Eq. (10) [9], assuming that the size of bubbles is sufficiently small. Also, it is assumed that the surface tension, and the conductivity and the pressure outside the bubble are constant.

$$p_s = \frac{\rho\ddot{v}}{4\pi d} \tag{10}$$

Here, p_s is the sound pressure that is instantaneously radiated at the distance "d".

From Eq. (8)~(9), it can be found that the radiated noise of the bubble is strongly related to the variation of its volume. And also, it can be found that the sizes of the bubble are strongly related to the flow pattern in a pipe when the phase of flow is 2-phase. Therefore, it can be expected to find the root causes of the refrigerant-induced noise through the bubble dynamics as well as 2-phase flow theory.

3. Estimation of the root causes of refrigerant-induced noise in refrigerators

As referred to in the previous paragraph, the refrigerant-induced noise in a refrigerator occurs when the state of the refrigerant in the pipe is two-phase. Considering the thermodynamic cycle of the refrigerator, the regions of two-phase flow are in the capillary tube, evaporator-inlet, evaporator, and condenser. Since the pipe layout is simple and the phase transition progresses gradually in the evaporator and condenser, the refrigerant-induced noise does not occur to any great extent in them. However, the refrigerant-induced noise occurs to a great extent in the region beginning

from the capillary tube-outlet till the evaporator-inlet because the bubbles that develop from the outlet of the capillary tube collapse, merge, and oscillate when they flow through the evaporator-inlet pipe.

The construction of the evaporator dealt in this section is shown in Fig. 3 and the operating refrigerant is R600a. In Fig. 3, the capillary tube is connected to the evaporator-inlet, which has a U-shaped tube. The diameter suddenly expands when the refrigerant exits the capillary and enters the evaporator-inlet tube. Considering the design of the evaporator-inlet pipe, it can be deduced that the refrigerant-induced noise can occur when the growing bubbles in 2-phase fluid flow into it.

Therefore, in the following section, the noise and vibration for the evaporator-inlet of the refrigerator are described in relation to the flow patterns and bubble dynamics.

3.1 The noise and vibration of the evaporator-inlet pipe

To define the characteristics of the noise of the refrigerator, the sound pressure and acceleration were measured, besides the cyclic temperature. The sound-pressure level was measured with a microphone, B&K type-4190, which was installed at the rear-side at 30 cm apart from the center of the refrigerator. The frequency range of the sound measurement was up to 12.8 kHz applying 7 Hz high pass filter. The cyclic temperature was measured with a T-type thermocouple and an Agilent 34970A data logger. Those data were collected every 1 second during the time the refrigerator was operating (120 minutes).

Firstly, the sound-pressure level was measured for the refrigerator at the rear-side when the compressor was alternatively switched on and off, as shown in Fig. 4. From Fig. 4, it can be noted that the range of the frequency of the refrigerant-induced noise is 250 to 2000 Hz, assuming that the noise from the compressor is sufficiently low.

Fig. 5 shows the variation of the cyclic temperature of the refrigerator with its operating time. From Fig. 5, it can be seen that the temperature (pressure) in the evaporator decreases and the mass quality increases with the passage of time. To determine the relationship between the noise and the cycle conditions, the sound-pressure level was measured simultaneously with the cyclic temperature and the mass quality. Fig. 6 shows the test results. As seen from Fig. 5, the noise fluctuated greatly from the start till about 30 minutes,

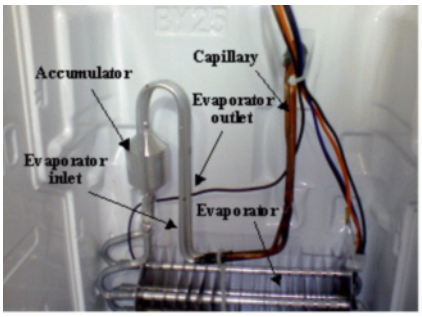

Fig. 3. Construction of the evaporator.

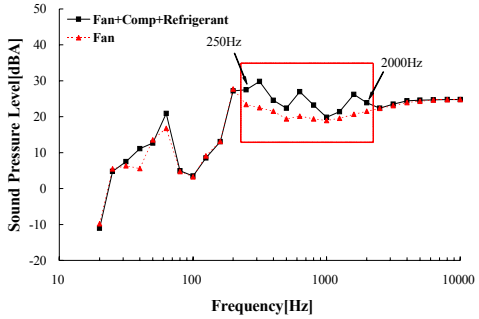

Fig. 4. Noises under normal operating condition and fan only operating condition.

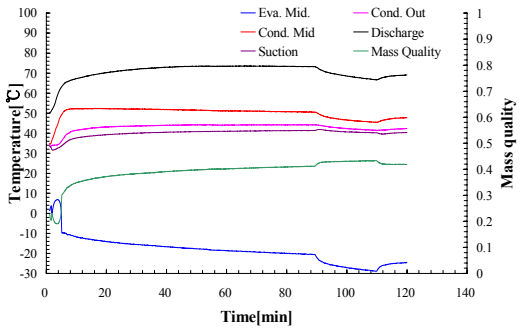

Fig. 5. The variations of the cyclic temperature and mass quality in the evaporator as time.

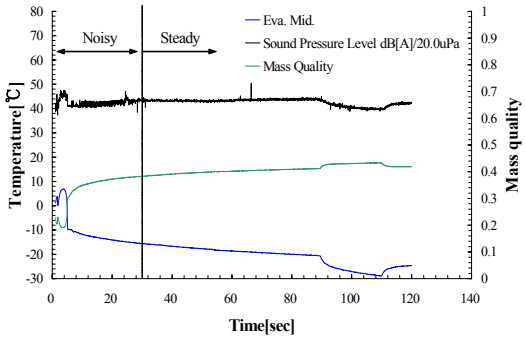

Fig. 6. Overall noise and temperature of the cycle.

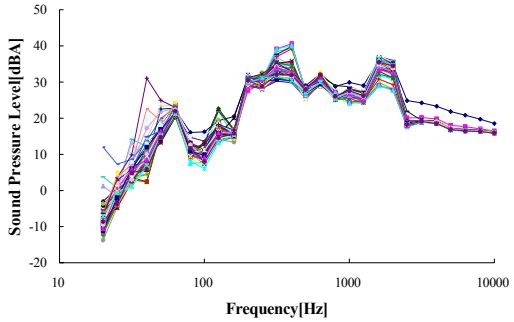

(a) 19~20 min. (for 60 sec)

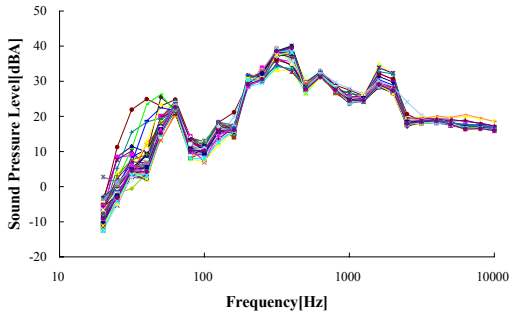

(b) 59~60 min. (for 60 sec)

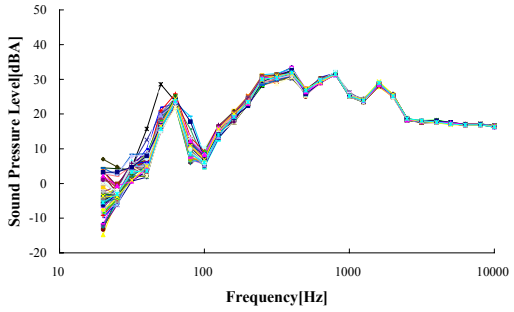

(c) 99~100 min. (for 60 sec)

Fig. 7. The variation of sound pressure level as time.

when the mass quality was 0.2~0.38 and the temperature of the evaporator was 8 ~ -16℃. The noise level remained steady from 30 to 90 minutes, when the mass quality was 0.38~0.42 and the temperature of the evaporator was -16~-20℃.

When the temperature of the evaporator decreased below -20℃ (after 90 minutes), the mass quality rapidly increased from 0.42 to 0.45 because of the variation of the thermodynamic cycle control. This implies the velocity in the evaporator-inlet increased and the sound-pressure level also increased. And, when the temperature of the evaporator was -20℃, the fan rpm increased in order to increase the amount of the heat transfer at the evaporator. It also implies that the sound-pressure level increased. However, in Fig. 5, the sound-pressure level was reduced even though the mass quality and fan rpm increased. From these test results, it can be deduced that the variation of the characteristics of the refrigerant, such as the flow pattern, should impact the noise.

Further, the variation of the 1/3 octave of the sound-pressure levels with the operating time was measured to define the characteristics of the refrigerant-induced noise in more detail, as shown in Fig. 7. The measured time of each spectrum was one second, and the spectra for 60 seconds are represented at a time in Fig. 7. From Fig. 7, it can be observed that the refrigerant-induced noise predominantly varied at two main frequency ranges until 30 minutes. The first range was from 315 Hz to 400 Hz and the other was from 1.6 kHz to 2 kHz. After 30 minutes, the degree of fluctuation of the sound-pressure level at these frequencies was reduced. After 60 minutes, the sound-pressure level became steady. In Fig. 7, the noise variation below 100 Hz was not considered here because of the performance limit of lower frequency in the anechoic chamber.

In addition to the noise test, the accelerations of the evaporator-inlet and outlet pipes were measured. Considering the gravity effect for the flow pattern at the vertical and horizontal pipe, the shape of bubbles should be different between them. Assuming that the noise from the bubble was dependent on its shape and it transferred the vibration to the pipe sufficiently, the accelerations for the horizontal and vertical pipe were measured, respectively.

Fig. 8 shows the acceleration on the evaporator-inlet and outlet pipes at the two main frequency ranges. Accelerometers of B&K type-4393 were installed on the horizontal and vertical pipes of the evaporator-inlet and outlet pipe, respectively. From Fig. 8, it can be seen that the acceleration level on the evaporator-inlet pipe was higher than that on the evaporator-outlet pipe.

Also, it can be noted that the acceleration level on the vertical pipe was higher than that on the horizontal pipe for the evaporator-inlet pipe. Through the assumption and results of the acceleration test, it can be deduced that the refrigerant-induced noise occurs mainly at the evaporator-inlet pipe and that the vertical pipe produces more refrigerant-induced noise than the horizontal pipe.

Table 1. Cycle variation of the refrigerator as operating time.

Time [min]	4	8	12	20	30	60	100
Temperature of evaporator-inlet [℃]	-10.3	-11.3	-12.5	-14.6	-16.4	-19.5	-28.7
Pressure of evaporator-inlet [Mpa]	0.1066	0.1026	0.09783	0.0899	0.0835	0.0736	0.0491
Diameter of the pipe [m]	0.00435	0.00435	0.00435	0.00435	0.00435	0.00435	0.00435
Mass flow rate [kg/hr]	2.8	2.8	2.8	2.8	2.8	2.8	2.8
Mass quality	0.28	0.31	0.33	0.34	0.36	0.38	0.41

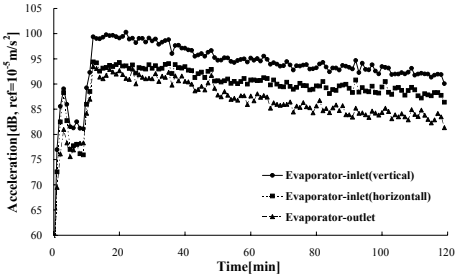

(a) 315 Hz

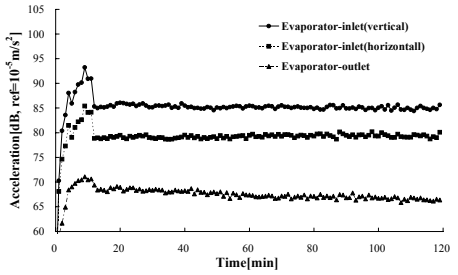

(b) 2000 Hz

Fig. 8. Acceleration on the evaporator inlet and outlet pipes.

3.2 Estimation of the flow pattern in an evaporator-inlet pipe

From the previous section, it can be seen that the refrigerant-induced noise occurs at the vertical pipe of the evaporator-inlet. Therefore, the flow patterns in the vertical pipe of the evaporator-inlet and the relationships between the flow pattern and the noise characteristics of the refrigerant are described in this section.

For the vertical flow, the characteristics of each flow pattern are as follows [10].

(1) Bubbly flow, in which the gas bubbles are approximately uniform in size.
(2) Plug flow or slug flow, in which the gas flows in the form of large, bullet-shaped bubbles.
(3) Churn (froth) flow, which is a highly unstable flow of an oscillatory nature. The liquid near the tube wall continually pulses up and down.
(4) Annular flow which is similar to the horizontal flow.

In this section, the flow patterns for the vertical tube of the evaporator-inlet pipe of the refrigerator are estimated through the flow-pattern map, as a function of the cycle variation of the refrigerator, as shown in Table 1.

The common flow patterns for the vertical flow in a round tube are shown in Fig. 9 [10]. Here, the Hewitt map [11], Taitel-Dukler map [12] and Oshinowo-Charles map [13] are used for estimating the flow pattern of the vertical flow.

Fig. 10 shows the flow-pattern estimation by the Hewitt map [11]. Generally, the flow pattern in a pipe has a strong relationship between the mass flux (mass flow rate per cross-section) of the gas and liquid.

When the mass flux of the gas is sufficiently larger than that of the liquid, the liquid is swept up to the surface of the pipe and it flows through the wall of the pipe. This kind of flow pattern is called annular flow. But, when it is not enough, the liquid falls to the bottom of the pipe and it makes a liquid bridge. It is called slug flow. When the mass flux of the liquid is more increased than that at the condition of slug flow, the velocity of the fluid in a pipe becomes slow and the gas bubbles having small diameter are formed in a liquid. It is called bubbly flow.

Therefore, in Hewitt map as given in Fig. 10, the flow pattern can be classified by the mass flux of gas and liquid, including other properties such as the density of gas and liquid. The cycle variations are the same as in the previous section. In Fig. 10, the flow pattern is estimated to be churn flow, when the mass quality is low. When the mass quality is over 0.4, the flow pattern is estimated to be annular.

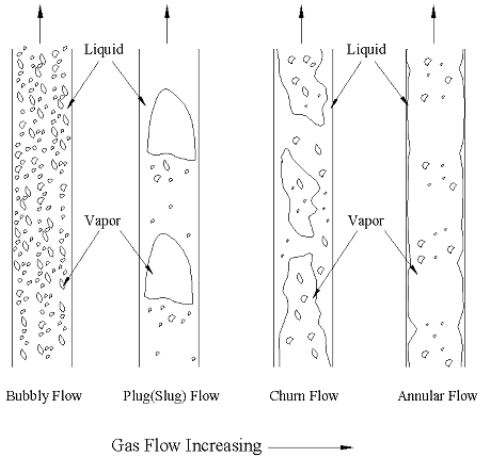

Fig. 9. Schematic diagram of flow pattern for vertical tube.

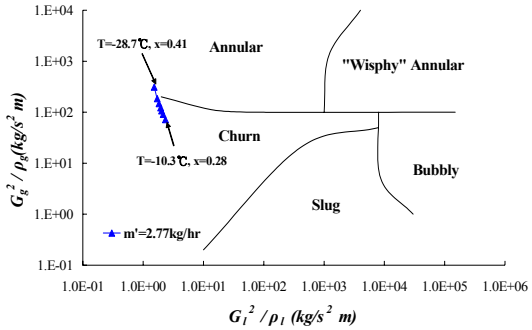

Fig. 10. Flow pattern estimation with Hewitt map.

In 1977, Taitel and Dukler suggested a flow-pattern map from the theoretical analysis of two-phase flow. The flow pattern has high relationship to the mass quality, which represents how much flow rate of the gas is in a pipe. Therefore, in order to classify the flow pattern, Taitel and Dukler used the Martinelli parameter represented by the mass quality, including other properties such as density and viscosity of the gas and liquid, which affect the flow pattern in a pipe as given in Eq. (11). At a typical Martinelli parameter, the flow pattern is transferred from slug (or churn) to annular flow when the Kutatelaze parameter of the gas as given in Eq. (12), which represents the superficial velocity of the gas including the other properties of the gas and liquid, increases. When the gas velocity increases due to increment of the gas flow rate, the liquid is swept up to the surface of the pipe and becomes annular flow. Based on this theory, the condition of transition from slug or churn to annular flow is given in Eqs. (11)~(13) [12].

$$X = \frac{(dp/dz)_f}{(dp/dz)_g} = \left(\frac{1-x}{x}\right)^{0.875}\left(\frac{\rho_g}{\rho_f}\right)^{0.5}\left(\frac{\mu_f}{\mu_g}\right)^{0.125} \tag{11}$$

$$Ku_g = j_g \rho_g^{1/2} / [g(\rho_f - \rho_g)\sigma]^{1/4} \tag{12}$$

$$Ku_g = 3.09 \frac{(1+20X+X^2)^{1/2} - X}{(1+20X+X^2)^{1/2}} \tag{13}$$

Here, X is the Martinelli parameter, Ku_g is the Kutatelaze parameter of the gas, j_g is the superficial velocity of the gas, g is the acceleration due to gravity and σ is the surface tension. Fig. 11 presents the results of estimation of the flow pattern with the Taitel-Dukler flow-pattern map [12] as the variations of the thermodynamic cycle conditions for the refrigerator in this research. In Fig. 11, the flow pattern is estimated to transit from slug or churn to annular flow with the passage of time when the mass quality is over 0.3.

Fig. 12 depicts the flow-pattern estimation by the Oshinowo-Charles flow-pattern map [13]. Oshinowo-Charles suggested by experiment that the flow patterns depend on the volumetric flow rate of the gas flow and other fluid dynamic properties similar to the other maps. Therefore, the flow pattern can be estimated through Eqs. (14)~(16) [13].

$$\beta = \frac{Q_g}{Q} \tag{14}$$

$$Fr = \frac{j^2}{gD} \tag{15}$$

$$\Lambda = \frac{\mu_l}{\mu_g}\left[\frac{\rho_l}{\rho_g}\left(\frac{\sigma}{\sigma_w}\right)^3\right]^{-1/4} \tag{16}$$

Here, β is the volumetric quality, Q_g is the volumetric flow rate of the gas, Q is the total volumetric flow rate, Fr is the Froude number, j is the superficial velocity, σ_W is the surface tension of the water and D is the diameter of the pipe. They suggested the flow pattern map for upstream and downstream, respectively, considering its shape such as a U-shaped tube. Here, the flow pattern map for the upstream is described only.

In Fig. 12, the flow pattern is estimated to transit from froth (churn) to annular flow when the mass quality is over 0.3, which is similar to the estimation through the Hewitt and Taitel-Dukler flow-pattern maps.

As described in the previous section, the refrigerant-induced noise occurs predominantly when the flow pattern in the pipe is intermittent. Therefore,

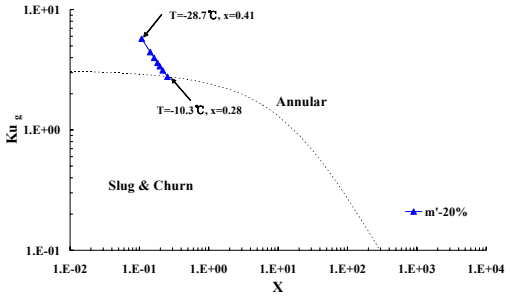

Fig. 11. Flow pattern estimation with Titel-Dukler map.

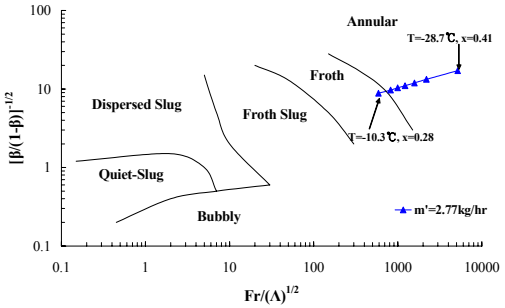

Fig. 12. Flow pattern estimation with Oshinowo-Charles map.

considering the flow patterns that are estimated through various flow-pattern maps, the refrigerant-induced noise may occur predominantly at the vertical tube of the evaporator-inlet pipe when the mass quality is low. And it can be known that this estimation is coincident with the test results in section 3.1.

The results of expectation for the flow patterns from Fig. 10~12 are very important in this research because the conditions transiting the intermittent flow to an annular one can be estimated with these flow pattern maps, and the methods can be found how the refrigerant-induced noise is reduced, assuming that they are strongly dependent upon the flow pattern.

In the next section, the frequency characteristics of these bubbles will be investigated with bubble dynamic theories.

3.3 Estimation of the frequency characteristics of the refrigerant-induced noise from the evaporator-inlet pipe

As described in section 3.1, the range of frequency of the refrigerant-induced noise is 250~2000 Hz. Theoretically, the frequency range of the noise for the spherical bubble can be estimated through the relationship between the size(radius) of the bubble and the resonance frequency.

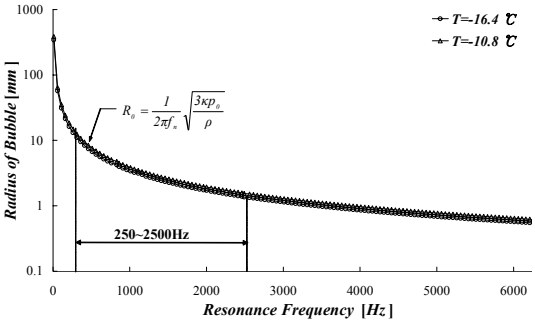

Fig. 13. Estimation of the bubble size from the resonance frequency of the bubbles.

Fig. 13 shows the bubble size that is estimated at this frequency range for the operating range of the refrigerator. It is calculated by Eq. (8) when the temperature of the evaporator is either -10.8℃ or -16.4℃. From Fig. 13, it can be noted that the bubble size is distributed from 1mm to 13mm at the given cycle conditions. The bubble sizes at 315 Hz and 2000 Hz, where the refrigerant-induced noise is very high, are estimated to be in the ranges, 10.8~12.3mm and 1.3~1.9mm, respectively, assuming that the shape of the bubble is spherical.

The bubbles whose radii are in the range of 10.8mm~12.3mm cannot be spherical in a pipe because the inner radius of the pipe is 2.175mm. Assuming that the spherical bubbles which have larger diameter than inner diameter of the pipe are changing their shape in order to keep up their volume, the length of bubbles should be long.

Reviewing the flow pattern in a vertical tube, as described in Fig. 9, the length of slug and churn bubble is considerably longer than the pipe diameter. Therefore, it can be seen that the estimated size of the bubbles whose radius is in the range of 10.8~12.3mm is similar to those of the slug and churn bubbles whose length is sufficiently long, viz., more than many times the inner diameter of the pipe.

And also, the slug and churn bubbles can collapse when they flow through the pipe and can have a diameter that is less than half the pipe diameter. These collapsing bubbles having a diameter less than the inner diameter tend to maintain their shape to be spherical because of surface tension. Therefore, the noise at the frequency range from 2 kHz can occur from the collapsing bubbles whose radii are in the range of 1.3~1.9mm.

Consequently, it can be inferred that the refrigerant-induced noise from the evaporator-inlet pipe is caused

by the slug or churn flow in the vertical line, given the results of the flow-pattern estimation as well as those of the estimation of bubble sizes.

Therefore, this inference will be verified with refrigerant supplying equipment in the next section.

4. Experimental verification

As mentioned in the previous section, it can be observed that the refrigerant-induced noise from the evaporator occurs because of the intermittent flow in the vertical pipe of the evaporator-inlet. To verify this estimation, equipment that supplies refrigerant to the evaporator is developed. This equipment can operate continuously at the typical cycle conditions where the refrigerant-induced noise occurs. Therefore, in this section, the estimated root causes of the refrigerant-induced noise are experimentally verified.

4.1 Test equipment and operating conditions

Fig. 14 shows the refrigerant-supplying equipment for the evaporator. As depicted in Fig. 14, the refrigerant is supplied to the evaporator of the test unit in an anechoic chamber by the refrigerant-supplying equipment. The test unit consists of the cabinet of the refrigerator, fan, and evaporator sans the condenser and compressor from the refrigerator. Therefore, when the refrigerant flows in the test unit, the noise is only dependent upon the flow of refrigerant in the evaporator assembly, assuming that the fan noise is constant. The cycle conditions are controlled by the condenser, expansion valve, sub-cooler, and heater in the refrigerant-supplying equipment, and the glass tubes are installed at the vertical tubes of the evaporator-inlet, so that the flow pattern can be inspected in them.

The tests are performed under the cycle conditions that are shown in Table 2. In Table 2, the tests are performed at various pressures of the evaporator, while the mass quality is varied from 0.2 to 0.7.

4.2 Sound measurement and flow-pattern visualization

To measure the sound that comes from the refrigerant, a microphone (B&K type-4190) was installed at the rear side of the test unit, as in the test setup for the refrigerator. When the sound was measured at the typical cycle conditions, the images of the flow pattern in the glass tube were simultaneously captured by a digital camcorder. Fig. 15 shows the variation of the flow pattern with the mass quality for the vertical tubes, when the temperature of the evaporator is -10℃.

Table 2. Test conditions for the refrigerant supplying equipment.

Temperature (℃)	Pressure (MPa)	Mass quality
-5	0.1304	0.2, 0.4, 0.6, 0.7
-10	0.1058	0.2, 0.4, 0.6, 0.7
-12.5	0.09783	0.3, 0.4, 0.5, 0.7

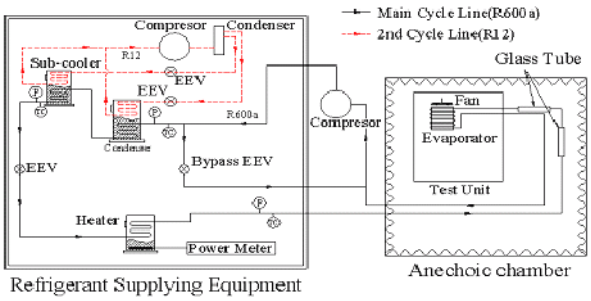

Fig. 14. Schematic diagram of the refrigerant supplying equipment.

In Fig. 15, it can be known that the flow pattern is churn flow at low mass quality(x=0.2) and annular flow at high mass quality(x=0.7). But when the mass quality is 0.4 and 0.6, it cannot be defined exactly whether it is annular or churn flow. Even though the visualization of the flow pattern does not accurately succeed, the transition of the flow pattern from churn to annular flow as increasing mass quality can be identified the same as the estimation of the flow pattern map. When the mass quality was in the range of 0.2~0.4, the bubbles whose diameter was less than that of the pipe could be inspected similar to the bubble size and frequency characteristics estimated in section 3.3. But the bubbles having long length could not be inspected accurately. However, it was inspected that the liquid-bridge appeared and disappeared repeatedly. At this time, it could be known that the noise at 315 Hz and 400 Hz was also increased.

Fig. 16 shows the variation of the 1/3 octave noise with the cycle conditions given in Table 2. The frequency of the refrigerant-induced noise can be discerned by comparing the noise when the refrigerant is flowing in a test unit with the noise when no refrigerant is flowing. Therefore, from Fig. 16, it can be seen that the main frequency ranges of the refrigerant-induced noise are 315 Hz and 2000 Hz, which are the

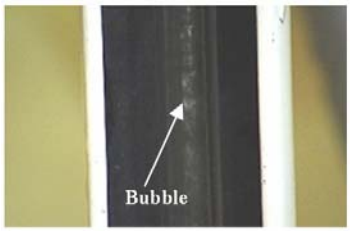

(a) x=0.2(churn)

(b) x=0.4(Annular or churn)

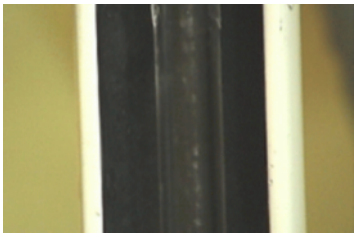

(c) x=0.6(Annular or churn)

(d) x=0.7(Annular)

Fig. 15. Pictures of the flow pattern in a glass tube according to the mass quality variations for vertical pipe (T = -10℃).

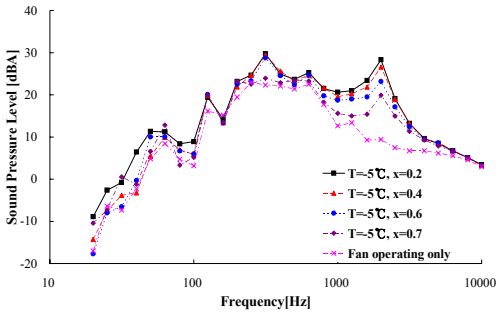

(a) Sound spectrum (T=-5℃)

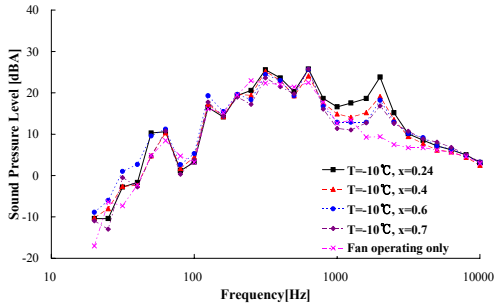

(b) Sound spectrum (T=-10℃)

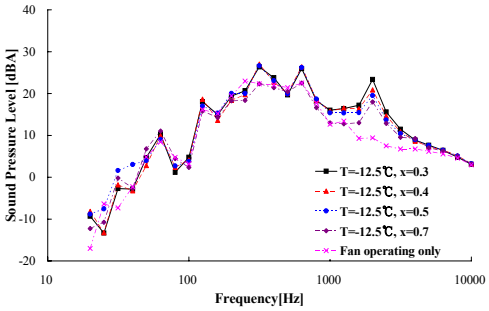

(c) Sound spectrum (T=-12.5℃)

Fig. 16. The spectrum of the sound for the test unit according to the variation of the mass quality and temperature in the evaporator.

same as in the refrigerator test. When the temperature of the evaporator is under -10℃, another noise peak appears at the 630 Hz frequency band as shown in Fig. 16(b) and (c), which are different as in the refrigerator test. It is inferred that the slug or churn bubbles having less length than those in the evaporator-inlet pipe of the refrigerator may have additionally occurred when the evaporator was tested with refrigerant-supplying equipment. Considering these frequency ranges of the refrigerant-induced noise, it can be observed that the sound-pressure level at this frequency range decreases as the mass quality increases, as shown in Fig. 16, for each cycle temperature and it can be verified that the flow patterns in a pipe are highly related to the refrigerant-induced noise.

Fig. 17 shows the estimations of the flow pattern for the vertical pipe at the test conditions listed in Table 2. Also, the noises at those states are simultaneously denoted on the flow-pattern map in Fig. 17. Here, “Noisy” implies that the irregular refrigerant-induced noise is serious. And “Quiet” denotes that refrigerant-induced noise does not seriously occur and the sound level is constant as time goes on.

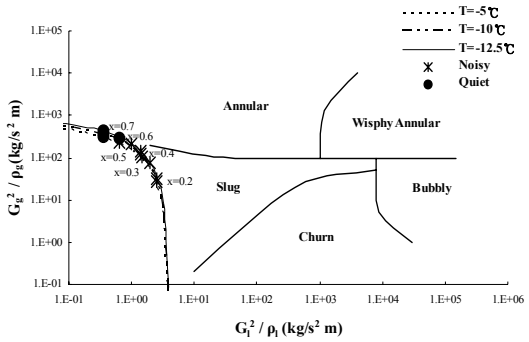

(a) Hewitt map

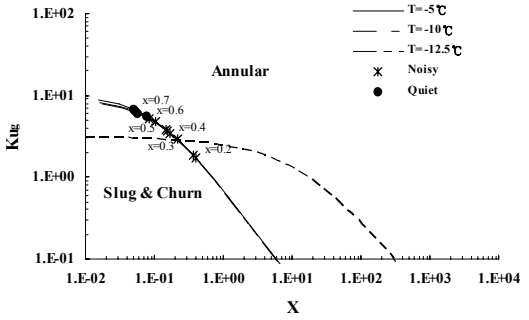

(b) Titel-Dukler map

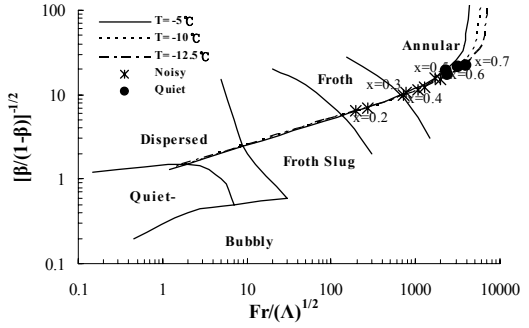

(c) Oshinowo-Charles map

Fig. 17. Flow pattern estimation by various flow pattern maps at the test conditions in Table 2.

Here, the evaluation of the noise such as "Noisy" and "Quiet" was performed by the researcher's subjective evaluation. Even though the inspected flow patterns are not exactly the same as those estimated by the flow-pattern maps, the phenomena of the transitions of the flow patterns and noise are similar in both cases, as is evident from Fig. 17.

In general, the noise from a bubble is inspected before the bubble can be visualized. When the initial bubbles occur, the pressure variation, including the sound pressure of the bubbles, can be measured even though it cannot be visualized. Therefore, a difference between the noise and flow pattern, as shown in Fig. 17, may occur because the flow pattern can possibly be the initial state of intermittent flow, even though it seems annular by visualization.

Considering these phenomena, there is some discrepancy between the estimations of the noise and the flow pattern by the flow-pattern map. Therefore, this difference should be investigated in future research.

Through the test results, it can be verified that the root cause of the irregular, refrigerant- induced noise comes from the bubbles that have an intermittent-flow pattern. Therefore, to avoid this kind of noise, flow patterns in a region of two-phase flow should be considered at the design step for avoiding the intermittent-flow pattern.

If it is possible for intermittent flow in a pipe to exist, it should be avoided by increasing mass flux through reducing diameter or increasing mass flow rate in order that the flow pattern be annular flow in a pipe.

5. Conclusion

From the theories of two-phase flow, including bubble dynamics and experiments, the root causes of the irregular, refrigerant-induced noise of the refrigerator can be identified as follows.

(1) The irregular, refrigerant-induced noise from the refrigerator occurs at the region of two-phase flow in an evaporator inlet pipe, especially a vertical pipe.

(2) The frequency ranges of the refrigerant-induced noise can be estimated by the resonance frequency of bubbles, and they can be verified by experiments with refrigerant-supplying equipment.

(3) When the flow pattern in an evaporator-inlet pipe is intermittent flow, the irregular, refrigerant-induced noise increases. However, when the flow pattern is steady, e.g., annular or wavy, the irregular, refrigerant-induced noise should be reduced.

(4) To eliminate the irregular noise from the refrigerant, the cycle conditions, such as the mass velocity and mass quality, should be considered so that an intermittent-flow pattern can be avoided in the evaporator inlet pipe.

In this research, several assumptions were applied in order to find the relationship between the bubbles from the 2-phase flow and refrigerant-induced noise. These assumptions can reduce the accuracy of the

results in this research. Therefore, they should be studied more in the future.

Acknowledgment

This research was financially supported by the Ministry of Education, Science Technology (MEST) and Korea Industrial Technology Foundation (KOTEF) through the Human Resource Training Project for Regional Innovation.

References

[1] S. Hirakuni, Noise Reduction Technology Caused by Refrigerant Two-Phase Flow for Room Air-Conditioner, *Japanese J. Multiphase Flow*. 18 (1) (2004) 23-30.

[2] S. Hirakuni, Y. Smida and H. Yamamoto, Study of Noise Reduction of Refrigerant for Capillary Tube in the Refrigerator, *32nd Conference Journal of Refrigeration and Air-Conditioning Association*. 4 (1998) 22-24.

[3] T. Umeda, Reduction of Noise Caused by Gas-Liquid Two-Phase Refrigerant Flow Through an Expansion Valve, *JSME*. 59 (557) (1993) 243-248.

[4] T. Kannon, Study on Noise Caused by Slug Flow through a Capillary Tube, *JSME*. 63 (611) (1997) 2392-2397.

[5] T. Umeda, Noise Caused by Gas-Liquid Two-Phase Flow with Single Large Gas Bubble through an Orifice(1st Report, Experimental Study Using Air-Water Two Phase Flow), *JSME*. 60 (574) (1994) 56-63.

[6] J. H. Park, Definition and Improvement of the Sound which was Generated by Bubbles at the Accumulator of the Evaporator, *KSNVE*. 6 (4) (1996) 513-519.

[7] S. Y. Lee, B. J. Kim and M. W. Kim, *Two-Phase Flow Heat Transfer*, Dae-Young Sa, Korea, (1993).

[8] W. K. Minnaert, On musical air bubbles and the sound of running water, *Phil. Mag.* (16) (1933) 235-248.

[9] M. Strasberg, Gas bubbles as source of sound in liquids, *The Journal of the Acoustical Society of America*. 28 (1) (1956) 20-27.

[10] P. B. Whalley, *Two Phase Flow and Heat Transfer*, Oxford University Press, New York, USA, (1999).

[11] G. F. Hewitt and D. N. Roberts, Studies of Two-Phase Flow Patterns by Simultaneous Flash and X-Ray Photography, *AERE-M2159*. (1969).

[12] Y. Taitel and A. E. Dukler, Flow Regime Transitions for Vertical Upward Gas-Liquid Flow: A Preliminary Approach Through Physical Modeling, *AIChE 70th Annual Meeting*, Session on Fundamental Research in Fluid Mechanics, New York, USA (1977).

[13] T. Oshimowo and M. E. Charles, Vertical Two-Phase Flow. Part 1, Flow Pattern Correlations, *Can. J. Chem. Eng*. 52 (1974) 25-35.

Hyung-Suk Han received a B.S. in Production and Mechanical Engineering from Pusan National University in 1996. He then went on to receive his M.S. and Ph.D. degrees from Pusan National University in 1998 and 2007, respectively. Dr. Han is currently a Senior Researcher at Defense Agency of Technology and Quality, Busan, Korea.

Weui-Bong Jeong received B.S. and M.S degrees from Seoul National University in 1978 and from KAIST in 1980, respectively. He then received his Ph.D. degree from Tokyo Institute of Technology in 1990. Dr. Jeong is currently a Professor at the Department of Mechanical Engineering at Pusan National University in Busan, Korea.

Min-Seong Kim received a B.S. in Mechanical Engineering from Pusan National University in 2007. He is currently a graduate student in Mechanical Engineering at Pusan National University in Busan, Korea.

Tae-Hoon Kim received his B.S. and M.S. in Mechanical Engineering from Pusan National University in 2003 and 2005, respectively. He is currently a Junior Research Engineer at LG Electronics co., Changwon, Korea.